High resolution imaging of the dolomite (104) cleavage surface by atomic force microscopy

Carlos M. Pina *, Carlos Pimentel, Marta García-Merino

Department of Crystallography and Mineralogy, Complutense University of Madrid, 28040 Madrid, Spain

Keywords:
Solid–liquid interfaces
Dolomite
Atomic force microscope

A B S T R A C T

In this paper we present high resolution atomic force microscopy (AFM) images of dolomite (104) cleavage surfaces immersed in pure water. These images show a rectangular lattice with surface unit cell dimensions in general agreement with those derived from the dolomite bulk structure. Furthermore, the two-dimensional fast Fourier transform (2D-FFT) plots of the high resolution images exhibit a pattern of periodicities consistent with both the alternate orientation of the carbonate groups and the positions for calcium and magnesium atoms on the dolomite (104) surface. However, the Mg^{2+} and Ca^{2+} sublattices could not be resolved. Finally, the images in both the real and the Fourier space do not reveal any clear evidence of reconstruction of the dolomite (104) surfaces.

1. Introduction

Dolomite ($CaMg(CO_3)_2$) is a widespread carbonate on the Earth's crust. This mineral has been found in numerous sedimentary formations and, together with calcite, plays an important role on the functioning of the so-called long term carbon cycle [1]. Despite its abundance in ancient sedimentary rocks, dolomite rarely forms in present aqueous environments and it is extremely difficult to synthesize at room temperature [2–4]. This is referred in the literature as the dolomite formation problem [5,6, and references therein], which has been frequently explained by the large differences in the dehydration activation energies of Ca^{2+} and Mg^{2+} ions and by the difficulty of an ordered and equal incorporation of these ions into growing surfaces [2,7,8].

Dolomite crystallises in the rhombohedral $R\bar{3}$ space group, with hexagonal cell parameters $a=0.4812$ nm, $c=1.6020$ nm, $\alpha=\beta=90.00°$, $\gamma=120.00°$, and $Z=4$ [9]. Its structure can be described as a calcite structure in which half of the Ca atoms are replaced by Mg atoms, resulting in an ordered compound. Although dolomite and calcite are structurally very similar, their reactivity in aqueous environments is remarkably different. While calcite (104) surfaces easily dissolve in water and grow from supersaturated solutions, the dissolution of dolomite (104) surfaces is slow and their growth from supersaturated solutions has found to be strongly inhibited [10–14].

In recent years, a considerable effort has been devoted to characterise dolomite (104)-water interfaces at a nanoscale using surface sensitive techniques. Higgins and Hu [14] have shown that continuous layer-by-layer growth from supersaturated solutions with respect to dolomite is inhibited on dolomite (104) after the formation of the first two monolayers. These authors attributed such a self-inhibiting growth to structural and/or compositional differences in the first dolomite monolayers. X-ray photoelectron spectroscopy studies indicate that such growth monolayers on dolomite (104) are Ca-rich. This result agrees with the slow dehydration kinetic of Mg^{2+} in comparison to that of Ca^{2+} [8]. Furthermore, lateral force microscopy studies of the newly-formed monolayers on dolomite (104) surfaces have revealed differences in friction forces that can be related to their enrichment in Ca and the associated structural changes [15]. In order to further characterise these compositional and structural changes, more detailed experimental studies of the surface structure of dolomite (104) in contact with aqueous solutions with different composition are required.

In this paper, we present, to the best of our knowledge, first high resolution atomic force microscopy (AFM) images of dolomite (104) surfaces immersed in pure water. The images obtained have nearly atomic resolution and their analysis revealed detailed structural features that can be compared to both the calcite (104) surface structure and the dolomite bulk structure. Therefore, these images can be a useful reference for future investigations on the dissolution and growth of dolomite (104) face at a nanoscale.

2. Materials and methods

2.1. The dolomite sample

The dolomite sample used in this work was of optical quality from Eugui, Navarra (Spain). The sample was confirmed to be dolomite by X-ray powder diffraction characterisation (Siemens D-500 using

* Corresponding author. Tel.: +34 913944879; fax: +34 913944872.
E-mail address: cmpina@geo.ucm.es (C.M. Pina).

Cu K-radiation). The obtained d-spacings of the five main dolomite planes are: $d_{104} = 0.2884$ nm, $d_{113} = 0.2193$ nm, $d_{202} = 0.2017$ nm; $d_{018} = 0.1805$ nm, and $d_{116} = 0.1786$ nm. These dolomite d-spacings are almost identical to those reported in the literature [9,16].

Dolomite (104) surfaces were also imaged by scanning electron microscopy (JEOL JSM 6400,40 kV) and analysed using a Link-analytical EDX. From the semi-quantitative EDX analysis of sample surfaces the following dolomite formula was calculated: $Mg_{0.88}Ca_{1.04}Mn_{0.01}Fe_{0.08}(CO_3)_2$.

2.2. AFM imaging of dolomite surfaces

Images of dolomite (104) surfaces were obtained using an atomic force microscope (Multimode Veeco Instruments) equipped with a ~14×14 μm² (E) scanner and a fluid cell. Dolomite crystals were cleaved with a blade razor parallel to the (104) face prior to be placed into the fluid cell of the AFM. Then deionised water (Milli-Q Millipore; resistivity 18 MΩcm) was injected. All high resolution AFM images shown in this paper were taken in contact mode while displaying the height signal. They were collected at scan rates which varied from ~20 Hz to ~60 Hz and 512 lines per scan. Scan areas varied from 5×5 nm² to 50×50 nm². Silicon nitride triangular tips with nominal force constants ranging from 0.06 to 0.58 N/m were used (Veeco DNP-S10). In order to both optimize the quality of the images and highlight different features of the dolomite (104) surface structure low and high pass filters, as well as different values for the z-limit and the integral and proportional gains, were used. A total number of about 560 images were collected.

2.3. Two-dimensional fast Fourier transform (2D-FFT) plots

A number of selected high resolution AFM images were converted into Fourier space using the two-dimensional fast Fourier transform (2D-FFT) algorithms included in the Nanoscope (5.30r3sr3) and Nanotec (WSxM. 2.1) software [17]. The construction of 2D-FFT plots was carried out from the raw data of images with sizes higher than 20×20 nm². These images are less distorted and have higher signal/noise ratios than smaller images. Therefore, they are more adequate to obtain more reliable values for surface periodicities [18]. Measurements conducted on 2D-FFT plots allowed us to determine surface cell parameters and to detect periodicities along main crystallographic directions on dolomite (104).

3. Results and discussion

Dolomite (104) surfaces in contact with water dissolve slowly. After a few minutes of injecting deionised water in the fluid cell of the AFM, only a slight retreat of cleavage steps and the formation of a few etch pits located on defective areas (e.g. scratches and outcrops of screw dislocations) occur. With time, the signs of dissolution become more evident and, about half an hour after initiating the dissolution experiment, a random distribution of etch pits can be observed. Then, dissolution proceeds by both the retreat of cleavage steps and the nucleation and coalescence of etch pits (see Fig. 1). Typical etch pits have a rhombohedral shape and a depth of ~0.3 nm. From goniometric measurements carried out on the AFM images of the etch pits, the main crystallographic directions on dolomite (104) surfaces can be determined. Once these directions were defined, we proceed to obtain high resolution images. Fig. 2a shows a typical high resolution AFM image of a dolomite (104) terrace. As can be seen in this figure, rows of bright spots run parallel to the [42$\bar{1}$] and [010] directions, defining a rectangular lattice (Fig. 2b). The conversion of 67 high resolution AFM images of dolomite surfaces into Fourier space and the subsequent measurement of the main periodicities along the [42$\bar{1}$] and [010] directions on the 2D-FFT maps yielded average surface lattice parameters of $a = 0.83 \pm 0.01$ nm and $b = 0.51 \pm 0.02$ nm, respectively (see Fig. 3). These parameters are in general agreement with the surface lattice parameters as obtained from the dolomite bulk structure (i.e. $a = 0.77$ nm and $b = 0.48$ nm). However, our measurements yielded larger a and b parameters than those calculated from the dolomite structure. This might be interpreted as a relaxation of the dolomite (104) surface, which would be then slightly more significant along the [42$\bar{1}$] direction (~7%) than along the [010] direction (~6%). Nevertheless, further experimental and computational work is needed to confirm such a surface relaxation.

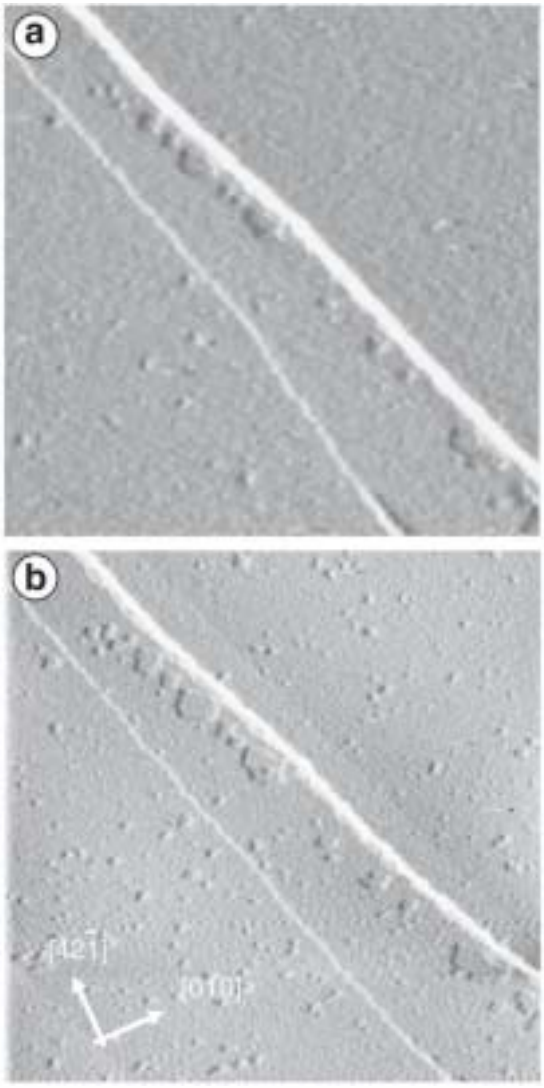

Fig. 1. AFM deflection images of a dolomite (104) surface in deionised water. (a) Surface about 40 minutes after starting the dissolution experiment. (b) The same surface 10 minutes later. Dissolution is evidenced by both the retreat of cleavage steps and the increase in the number and the size of shallow etch pits (~0.3 in depth). The [42$\bar{1}$] and [010] crystallographic directions are indicated by white arrows. (Size of both images: 2×2 μm²).

The patterns that we observed in a number of high resolution AFM images of dolomite (104) surfaces obtained under different operation conditions (e.g. scan sizes and angles, integral and proportional gains, and filters) are very similar to those reported for calcite (104) surfaces by Rachlin et al. [19], and more recently by Rode et al. [20]. This allowed us to relate features of the high resolution images of the dolomite (104) surfaces to structural characteristics shared by the calcite and dolomite surfaces.

Rode et al. [20] observed a zigzag sequence of bright spots along the [42$\bar{1}$] direction on calcite (104) surface that can be clearly

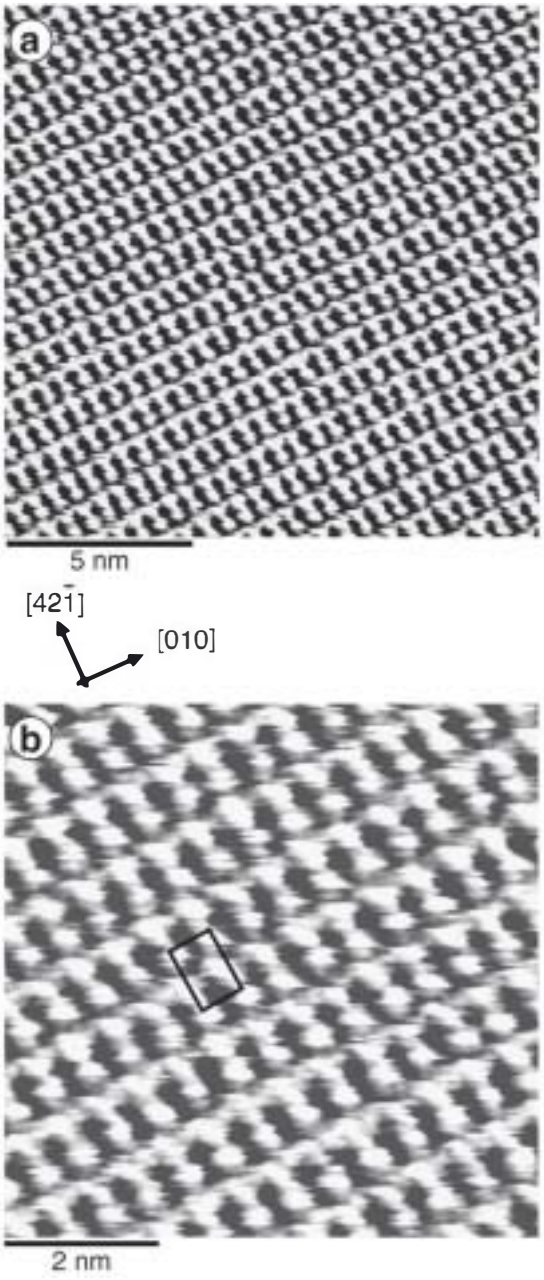

Fig. 2. (a) High resolution AFM image of dolomite (104) face in deionised water. This image was taken at a scan rate of 61 Hz and low pass (1) and high pass (3) filtering were used. (b) Detail of (a) showing the dolomite surface unit cell. White spots correspond to protruding oxygens belonging to carbonate groups with distinct orientations. Crystallographic directions are indicated by black arrows and they are valid for (a) and (b).

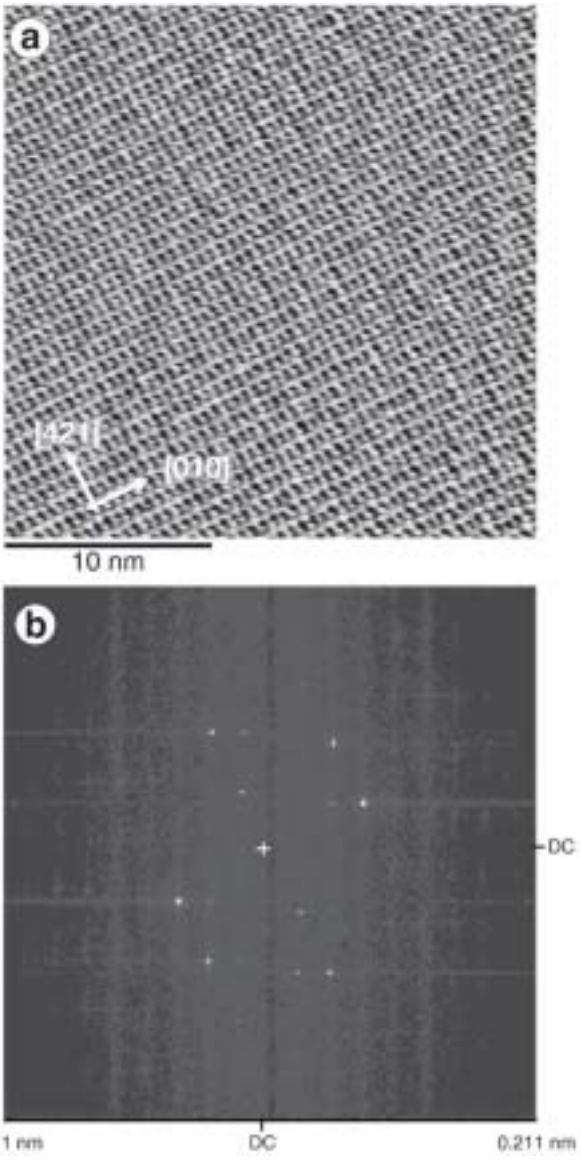

Fig. 3. (a) High resolution AFM image of dolomite (104) face in deionised water (scan rate: 61 Hz; low pass (1) and high pass (3) filtering used). (b) 2D-FFT plot of image (a) showing periodicities along the [42$\bar{1}$] and [010] directions. Crystallographic directions are indicated by black arrows and they are valid for (a) and (b).

attributed to the protruding oxygens of the carbonate groups. On the dolomite (104) surfaces we have observed an identical sequence of spots along the same direction. The periodicity of such spots measured on 2D-FFT plots is ~0.4 nm, in good agreement with the distance between successive carbonate groups with alternate orientation along the [42$\bar{1}$] direction on dolomite (104) surfaces (see Figs. 4 and 5). In the dolomite structure, along the [42$\bar{1}$] direction not only carbonate groups with alternate orientation are found but also Ca^{2+} and Mg^{2+} cations alternate with identical periodicity (Fig. 5). This makes especially difficult to image the two Ca^{2+} and Mg^{2+} sublattices on the dolomite (104) surface. In fact, none of the AFM images analysed revealed any significant difference in the cationic positions when compared with the high resolution images of calcite (104) surfaces [20]. Along the [42$\bar{1}$] direction we have not found changes in the shape or intensity of spots that could be clearly attributed to the alternating Ca^{2+} and Mg^{2+} and/or local differences in hydration on dolomite (104) surfaces. Since spatial differences in contrast in high resolution images of flat areas result from changes in distinct forces between the AFM tip and the atoms of the surface (e.g. repulsion of overlapping electron clouds and electrostatic interaction and frictional forces) [21], the undistinguishable cationic positions and their nearest spots indicate that Ca^{2+} and Mg^{2+} have a similar crystallochemical and hydration behaviour on the dolomite (104) surface. Nevertheless, in order to resolve the Ca^{2+} and Mg^{2+} sublattices and their distinct hydration, further experimental work using techniques such as frequency modulation AFM in liquids are required.

Along dolomite [010] direction straight sequences of bright spots are found. These spots correspond again to the protruding oxygens which belong to rows of carbonate groups (see Figs. 4 and 5). Differently to the [42$\bar{1}$] direction, along each [010] row, the carbonate groups have the same orientation. However, the orientation of carbonate groups alternate in successive [010] rows. The periodicity

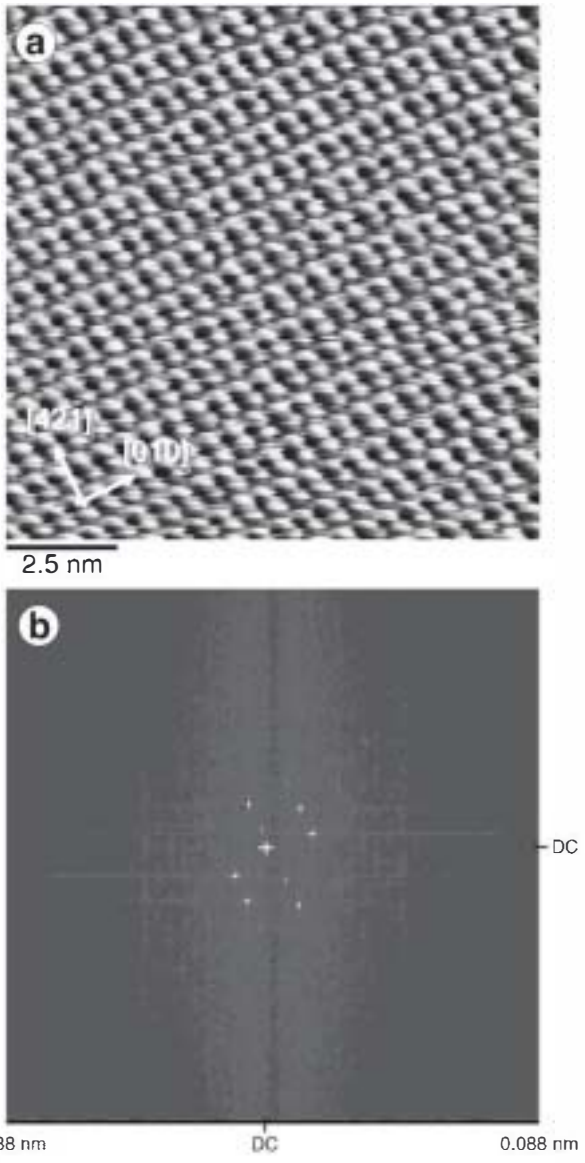

Fig. 4. (a) High resolution AFM image of dolomite (104) face in deionised water (scan rate: 61 Hz; low pass (1) and high pass (3) filtering used). In this image, bright and contrast have been optimised to enhance the zigzag and straight sequences of bright spots along the [42$\bar{1}$] and [010] directions, respectively. (b) 2D-FFT plot of image shown in (a). The crystallographic directions are indicated by black arrows and they are valid for (a) and (b).

of spots along the [010] direction measured on the 2D-FFT plots is 0.51 ± 0.02 nm, coinciding with the *b* surface lattice parameter.

Stipp et al. [21] analysed high resolution AFM images of calcite (104) surfaces and reported on a modulation along the [010] direction with periodicity of ~1 nm, resulting in a (2×1) superstructure (i.e. doubling the surface unit cell in the *b* dimension) that has been ascribed to a slight rotation of some surface carbonate groups. While the (2×1) superstructure on calcite (104) face matches with low-energy electron diffraction [22] and computer modelling studies [23,24], it has not been observed by Rode et al. [20] using frequency modulation AFM.

In the high resolution AFM images of dolomite (104) surfaces, we did not observe any variation in both the shape and the intensity of the spots that could be clearly attributed to the rotation of some carbonate groups along the [010] direction. In addition, the 2D-FFT plots obtained from these images did not reveal any clear evidence of a (2×1) superstructure on the dolomite (104) surface.

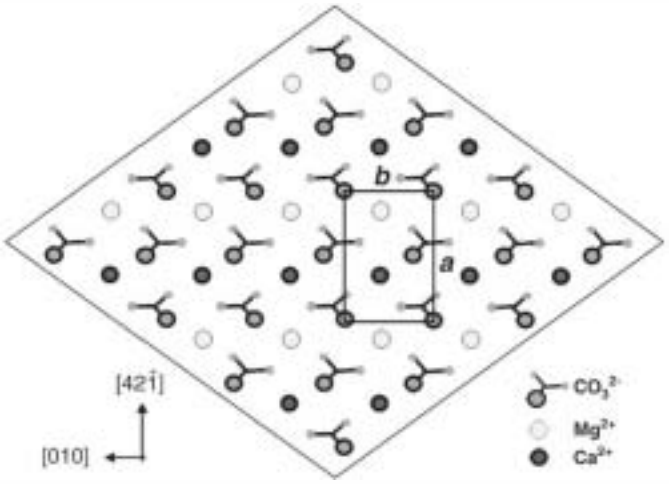

Fig. 5. The structure of the dolomite (104) cleavage surface. The rectangular surface unit cell has been drawn considering the periodicity of the protruding oxygens of the carbonate groups. These protruding oxygens have been represented by larger circles following the convention by Rode et al. [20].

4. Conclusions

The results of our investigation yielded new information on the nature of the dolomite-water interfaces. The high resolution AFM images of dolomite (104) surfaces immersed in water presented in this paper are very similar to those previously reported for calcite (104) face. Furthermore, the surface lattice parameters and the periodicities observed in the 2D-FFT plots are in good agreement with the structural features of dolomite (104) surface as derived from the bulk structure. However, the inspection of the AFM images and the corresponding 2D-FFT plots did not allow us to resolve the Ca^{2+} and Mg^{2+} sublattices. This could be partially due to the fact that the alternation of both the carbonate groups with opposite orientation and the Ca^{2+} and Mg^{2+} cations occurs with identical periodicity along the [42$\bar{1}$] direction. Moreover, in the 2D-FFT plots of the images, no modulations along the [010] direction in agreement with a possible (2×1) superstructure were observed. Both the identification of Mg–Ca ordering and possible superstructures on dolomite (104) surfaces require further experimental work and computer modelling efforts.

Acknowledgments

This work was financially supported by the Universidad Complutense-Comunidad de Madrid (Grant No. 910148-Superficies Minerales). The authors thank the Centro de Microscopia (UCM) for kindly providing them access to the AFM. The manuscript has been improved by the helpful comments of José M. Llorens and two anonymous reviewers.

References

[1] R.A. Berner, A.C. Lasaga, R.M. Garrels, American Journal of Science 283 (1983) 641.
[2] R.B. De Boer, Geochimica et Cosmochimica Acta 41 (1977) 265.
[3] R.S. Arvidson, F.T. Mackenzie, Aquatic Geochemistry 2 (1977) 273.
[4] R.J. Reeder, Estudios Geológicos 38 (1982) 179.
[5] R.S. Arvidson, F.T. Mackenzie, American Journal of Science 299 (1999) 257.
[6] D.T. Wright, D. Wacey, Geological Society of London 235 (2004) 65.
[7] P. Hartman, Neues Jahrbuch fuer Mineralogie Monatshefte 2 (1982) 84.
[8] D.K. Nordstrom, L.N. Plummer, D. Langmuir, E. Busenberg, H.M. May, American Chemical Society 416 (1990) 398.
[9] H. Effenberger, K. Mereiter, J. Zemann, Zeitschrift fuer Kristallographie 156 (1981) 233.
[10] P.E. Hillner, A.J. Gratz, S. Manne, P.K. Hansma, Geology 20 (1992) 59.
[11] H.H. Teng, P.M. Dove, J.J. De Yoreo, Geochimica et Cosmochimica Acta 64 (2000) 2255.
[12] H.H. Teng, Geochimica et Cosmochimica Acta 68 (2004) 253.
[13] X. Hu, D.A. Grossie, S.R. Higgins, American Mineralogist 90 (2005) 963.
[14] S.R. Higgins, X. Hu, Geochimica et Cosmochimica Acta 69 (2005) 2085.

[15] S.R. Higgins, X. Hu, P.F. Langmuir, American Chemical Society 23 (2007) 8903.
[16] R.J. Reeder, H.R. Wenk, American Mineralogist 68 (1983) 769.
[17] I. Horcas, R. Fernández, J.M. Gómez-Rodríguez, J. Colchero, J. Gómez-Herrero, A.M. Baró, Review of Scientific Instruments 78 (2007) 013705.
[18] D.G. Bokern, W.A.C. Ducker, K.A. Hunter, K.M. McGrath, Journal of Crystal Growth 246 (2002) 139.
[19] A.L. Rachlin, G.S. Henderson, M.C. Goh, American Mineralogist 77 (1992) 904.
[20] S. Rode, N. Oyabu, K. Kobayashi, H. Yamada, A. Kühnle, Langmuir 25 (2009) 2850.
[21] S.L.S. Stipp, C.M. Eggleston, B.S. Nielsen, Geochimica et Cosmochimica Acta 58 (1994) 3023.
[22] R. Kristensen, S.L.S. Stipp, K.J. Refson, Chemical Physics 121 (2004) 8511.
[23] A.L. Rohl, K. Wright, J.D. Gale, American Mineralogist 88 (2003) 921.
[24] A. Villegas-Jiménez, A. Mucci, M.A. Whitehead, Langmuir 25 (12) (2009) 6813.